Journal of Engg. Research Vol. 7 No. (4) December 2019 pp. 343-357

Modeling of the Reed Valves in Reciprocating Compressors and Investigation of Their Dynamics Characteristics

Guangyu Mu*,**, Feng Wang*** and Xiaozhen Mi****

**Mechanical and Power Engineering College, Dalian Ocean University, China*
***Mechanical Engineering College, Dalian JiaoTong University, China*
****Motor Train College, Dalian JiaoTong University, China.*
*****Traffic and Transportation College, Dalian JiaoTong University, China*
****Corresponding Author: wfmgy@hotmail.com*

ABSTRACT

In order to study the dynamics characteristics of the reed valve in reciprocating compressor, a new model based on energy conservation and Newton's second law of motion was developed in this study. In this new model, the structural parameters of the reed valve and the gas damping force are considered. Moreover, an experimental system of reciprocating compressor was established to measure the actual movements of the reed valve and evaluate the validity of the model. The simulation was implemented in a MATLAB environment for an efficient numerical solution and result presentation. The experimental results are consistent with the numerical simulation results, which show that the theoretical model proposed is effective and accurate. Furthermore, this study also used such model to analyze the effect of the structural parameters on dynamic characteristics. In practice, this paper can provide a beneficial reference for the optimization design of the reed valve.

Keywords: Reciprocating compressor; reed valve; dynamics characteristics; numerical simulation.

INTRODUCTION

Reed valves are the key components of reciprocating compressor, which can influence the efficiency and reliability of machines. In recent years, reed valves are widely used in micro air compressors and small refrigeration compressors due to its features of simple structure, light weight, and low cost (Wang Feng *et al.*, 2016). As shown in Figure 1, reed valves are mainly composed of a valve seat, a reed valve, and a lift limiter. In addition, reed valves can also control the flow of inlet and outlet gas automatically depending on the pressure difference between cylinder and suction/discharge chamber. The dynamics characteristics of the reed valve are that it has a direct impact on opening and closing time, fully open period, impact speed, and flutter. Besides, it also has an important impact on energy consumption. The flow resistance loss can be reduced to 3%-7% of compressor shaft power depending on well-designed valve (Yuan Ma *et al.*, 2012). Therefore, it is very necessary to study the dynamics characteristics of the reed valve for improving the working efficiency of compressor.

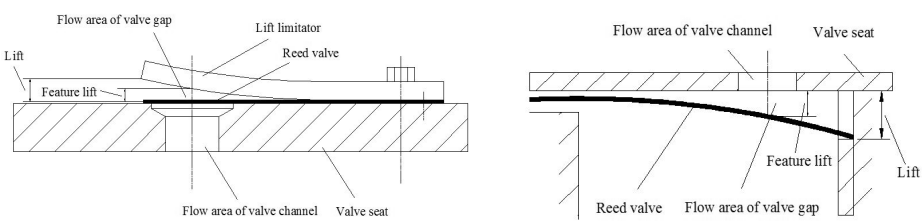

(a) Discharge valve component (b) Suction valve component

Fig. 1. The scheme of a reed valve component.

The dynamics characteristics of compressor valves have been studied by many scholars. Costagliola, M *et al*. (1950) first proposed the dynamics model to describe the valve motion in form of a single-degree of the freedom system. Wambsganss, M. W (1966) proposed a mathematical model to describe the valve motion in form of a bending beam. The calculated results were in good agreement with the experimental results at that time. Soedel Werner (1972) presents a dynamic model for valves to evaluate the performance of compressor. The first law model together with ideal gas state equation is applied in valve dynamic simulation for reciprocating compressor in one thermal cycle. Soedel Werner (1984) systematically introduces the ideas and methods of valve design, including the calculation method of the effective flow area, the simulation of valve motion, valve reliability, energy loss, and so on. Lawson, S *et al.* (1984) carry out a dynamic numerical simulation of the reed valve, which takes the influence of valve gap pressure drop into account. Lin Mei *et al*. (1997) established a single-degree freedom model for the reed valve and believe that the model is both accurate and convenient. Machu, E (2001) proposes a multi-degree of the freedom model based on D'Alembert's principle. In this model, the mutual influence of rotating motion and the translational motion of valve were considered. Bo Huang (2008) established a finite element model of the reed valve based on plate theory. The stress distribution of the valve under the maximum load was analyzed. Hong, W *et al*. (2009) proposed a dynamic model of compressor valve based on L-K real gas state equation. The thermal cycle of the reciprocating compressor is studied under the condition of stepless regulation.

Moreover, there are also many scholars who have conducted many experimental researches on the reed valve motion. Junghyoun Kim (2006) discovers that the dynamic behavior of valve is closely related to its natural frequency and the actual frequency is greater than the natural frequency. Daniel Nagy *et al*. (2008) point out that laser Doppler instrument can be used to measure the valve displacement and the measuring error of the device was within 2%. Shuhei NAGATA (2010) measures the dynamics characteristics of a suction valve using strain gauge. The results show that the maximum displacement of the suction valve is increased with the acceleration of compressor.

In this paper, a dynamic model of the reed valve based on energy conservation and Newton's second law of motion is developed. In the model, several structural parameters of the reed valve are considered. Afterwards, an experimental system is established to evaluate the validity of the model and the simulation is implemented in a MATLAB environment. Then the effects of the structural parameters on dynamic characteristics are analyzed.

DYNAMIC MODEL OF REED VALVES

Currently, the mathematical model of the description of valve motion is established based on the model of the ring valve and the mesh valve. However, since the reed valve is flexible but the ring valve is not, there must be some calculation error when using the model. In order to solve this problem, a new model based on energy conservation and Newton's second law of motion is developed. In the new model, the structural parameters such as valve lift, stiffness coefficient, effective flow area, and gas damping force are considered.

Gas flow differential equation of suction and discharge process

The following hypotheses are adopted during the process of model derivation (Wu Danqing *et al*., 1993):

(1) The Gas is regarded as the ideal gas in the compressor. The thermodynamic parameters of the working medium in the cylinder are uniform. Suction pressure and discharge pressure are the working pressure of the evaporator and condenser, respectively, under the standard operating conditions.

(2) Gas flow is regarded as an adiabatic steady flow. The influence of gas damping force and lubricating oil viscosity on valve is ignored.

(3) The heat exchange between the gas and the cylinder wall is ignored. Potential energy and kinetic energy of the gas in the cylinder are not taken into account.

(4) The influence of suction and discharge pressure pulsation on the compressor flow field is ignored. The influence of the leakage of working medium and lubricating oil on working chamber volume and working fluid state is ignored.

According to assumptions and energy conservation law above, equation 1 can be obtained:

$$dp + kp\frac{dV}{V} + kpv\frac{dm}{V} = 0 \tag{1}$$

where p is the transient pressure in cylinder, k is the specific heat ratio, V is the transient volume, v is the specific volume, and m is the gas quality in cylinder.

The orifice mass flow equation can be expressed as equation 2:

$$dm = \frac{\alpha_v A_v \sqrt{\frac{2kRT}{k-1}} \sqrt{1-(\frac{p_d}{p})^{\frac{k-1}{k}}}}{v_d} dt \tag{2}$$

where α_v is the flow coefficient of valve, A_v is the cross sectional area of valve gap, R is the ideal gas constant, T is the transient temperature, p_d is the discharge pressure, v_d is the specific volume of discharge chamber, and t is the time.

According to equation 2 and equation 1, the flow differential equation of discharge process can be expressed as equation 3:

$$dp + \frac{kpdV}{V} + \frac{kp}{V}(\frac{p_d}{p})^{\frac{1}{k}} \alpha_v A_v \sqrt{\frac{2kRT_d}{k-1}((\frac{p}{p_d})^{\frac{k-1}{k}} - 1)} dt = 0 \tag{3}$$

where T_d is the discharge temperature.

The pressure ratio (ψ) can be expressed as equation 4:

$$\psi = \frac{p}{p_d} \tag{4}$$

According to equation 3 and equation 4, equation 5 can be obtained:

$$d\psi + k\psi\frac{dV}{V} + \frac{k}{V}\alpha_v A_v \psi^{\frac{k-1}{k}} \sqrt{\frac{2kRT_d}{k-1}(\psi^{\frac{k-1}{k}} - 1)} = 0 \tag{5}$$

According to the kinematics of the crank-slider mechanism, the relationship between displacement of piston working (x) and crank angle (θ) can be expressed as equation 6. The kinematics of the crank-slider mechanism is shown in Figure 2:

$$x = r(1-\cos\theta) + l(1-\sqrt{1-\lambda^2\sin^2\theta}) \tag{6}$$

where r is the crank radius, l is the length of the connecting rod, and λ is the crankshaft-connecting road ratio.

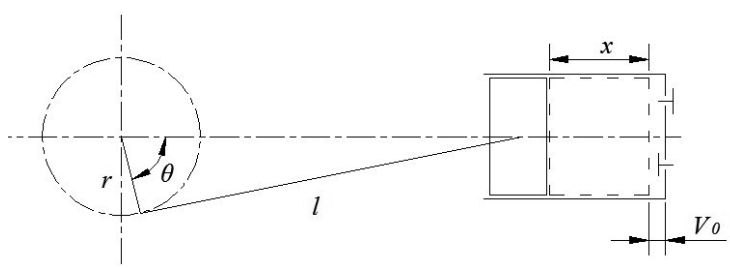

Fig. 2. The kinematics of the crank-slider mechanism.

Based on the Taylor series expansion, equation 6 can be simplified as equation 7:

$$x = r(1-\cos\theta+\frac{\lambda}{2}\sin^2\theta) \tag{7}$$

The transient volume (V) can be expressed as equation 8:

$$V = V_0 + S_p x \tag{8}$$

where V_0 is the clearance volume of cylinder and S_p is the piston area.

The relationship between the transient volume (V) and crank angle (θ) can be expressed as equation 9 and equation 10:

$$V=V_h\left(\xi+\frac{1-\cos\theta}{2}+\frac{\lambda}{4}\sin^2\theta\right) \tag{9}$$

$$\frac{dV}{d\theta}=V_h\left(\frac{\sin\theta}{2}+\frac{\lambda}{4}\sin 2\theta\right) \tag{10}$$

where V_h is the stroke volume of the piston, and ξ is the relative clearance volume of the cylinder.

According to equations 5, 9, and 10, the gas flow differential equation of discharge process can be expressed as equation 11:

$$\frac{\mathrm{d}\psi}{\mathrm{d}\theta}=-\frac{\left[\frac{1}{2}\omega\psi kV_h\sin\theta+\frac{\lambda}{4}\omega\psi kV_h\sin 2\theta+\psi^{\frac{k-1}{k}}\alpha_v\pi d_{dv}h_{dv}\sqrt{\frac{2kRT_d}{k-1}(\psi^{\frac{k-1}{k}}-1)}\right]}{\omega V_h(\xi+\frac{1}{2}-\frac{1}{2}\cos\theta+\frac{\lambda}{4}\sin^2\theta)} \tag{11}$$

where ω is the angular velocity, d_{dv} is the discharge orifice diameter, and h_{dv} is the transient displacement of the discharge valve.

Similarly, the gas flow differential equation of suction process can be expressed as equation 12:

$$\frac{d\varphi}{d\theta}=-\frac{\left[\frac{1}{2}\omega k\varphi V_h\sin\theta+\frac{\lambda}{4}\omega\varphi kV_h\sin 2\theta-\varphi^{\frac{1}{k}}\alpha_v\pi d_{sv}h_{sv}\sqrt{\frac{2kRT_s}{k-1}}\sqrt{1-\varphi^{\frac{k-1}{k}}}\right]}{\omega V_h(\xi+\frac{1}{2}-\frac{1}{2}\cos\theta+\frac{\lambda}{4}\sin^2\theta)} \tag{12}$$

where φ is the ratio of transient pressure in cylinder to suction pressure, d_{sv} is the suction orifice diameter, h_{sv} is the transient displacement of the suction valve, and T_s is the suction temperature.

Equation of motion of the Reed Valve

Lin Mei *et al*. (1997) point out that a single-degree of freedom model can effectively describe the reed valve motion. Therefore, in this paper the equation of the motion of the reed valve is established based on a single-degree of freedom model. Reed valves are affected by gravity, elastic force, gas force, gas damping force, and oil viscosity force at work. According to Newton's second law of motion, equation 13 can be obtained:

$$m_{dv}\frac{d^2h_{dv}}{dt^2}=F_g-F_{sp}+G-F_z-F_n \tag{13}$$

where m_{dv} is the equivalent mass of the discharge valve, F_g is the gas force, F_{sp} is the elastic force of valve, G is the valve gravity, F_z is the gas damping force, and F_n is the oil viscosity force.

The gas force (F_g) can be expressed as equation 14:

$$F_g = \delta \frac{\pi d_{dv}^{\ 2}}{4} p_d(\psi - 1) \tag{14}$$

where δ is the gas thrust coefficient. δ can be expressed as equation 15:

$$\delta = \alpha_v^{\ 2}(\frac{1}{\alpha_l^{\ 2}} + 1) \tag{15}$$

where α_l is the flow coefficient of the valve gap.

The elastic force (F_{sp}) can be expressed as equation 16:

$$F_{sp} = K_{dv} h_{dv} \tag{16}$$

where K_{dv} is the stiffness coefficient of the discharge valve.

The gas damping force (F_z) can be expressed as equation 17:

$$F_z = C \frac{dh_{dv}}{d\theta} \tag{17}$$

where C is the gas damping coefficient.

Since gravity (G) and oil viscous force (F_n) acting on the reed valve are much smaller than elastic force (F_{sp}) and gas force (F_g), they can be ignored for analysis convenience. According to equations 13, 14, 16, and 17, the equation of motion of the discharge valve can be expressed as equation 18:

$$\frac{d^2 h_{dv}}{d\theta^2} = \frac{1}{m_{dv}\omega^2}\left[\delta \frac{\pi d_{dv}^{\ 2}}{4} p_d(\psi - 1) - K_{dv} h_{dv} - C \frac{dh_{dv}}{d\theta}\right] \tag{18}$$

where ω is the angular velocity.

Similarly, the equation of motion of the suction valve can be expressed as equation 19:

$$\frac{d^2 h_{sv}}{d\theta^2} = \frac{1}{m_{sv}\omega^2}\left[\delta \frac{\pi d_{sv}^{\ 2}}{4} p_s(1 - \varphi) - K_{sv} h_{sv} - C \frac{dh_{sv}}{d\theta}\right] \tag{19}$$

where h_{sv} is the transient displacement of the suction valve, m_{sv} is the equivalent mass of the suction valve, p_s is the suction pressure, and K_{sv} is the stiffness coefficient of the suction valve.

Finally, the dynamic model of the discharge valve can be expressed as equations 20:

$$\left.\begin{aligned} &\frac{dh_{dv}}{d\theta} = y \\ &\frac{d^2 h_{dv}}{\mathrm{d}\theta^2} = \frac{1}{m_{dv}\omega^2}\left[\delta \frac{\pi d_{dv}^{\ 2}}{4} p_d(\psi - 1) - K_{dv} h_{dv} - C \frac{dh_{dv}}{d\theta}\right] \\ &\frac{\mathrm{d}\psi}{\mathrm{d}\theta} = -\frac{\left[\frac{1}{2}\omega\psi k V_h \sin\theta + \frac{\lambda}{4}\omega\psi k V_h \sin 2\theta + \psi^{\frac{k-1}{k}} \alpha_v \pi d_{dv} h_{dv} \sqrt{\frac{2kRT_d}{k-1}(\psi^{\frac{k-1}{k}} - 1)}\right]}{\omega V_h(\xi + \frac{1}{2} - \frac{1}{2}\cos\theta + \frac{\lambda}{4}\sin^2\theta)} \end{aligned}\right\} \tag{20}$$

Similarly, the dynamic model of the suction valve can be expressed as equations 21:

$$\left.\begin{aligned}
&\frac{dh_{sv}}{d\theta} = y \\
&\frac{d^2h_{sv}}{d\theta^2} = \frac{1}{m_{sv}\omega^2}\left[\delta\frac{\pi d_{sv}{}^2}{4}p_s(1-\varphi) - K_{sv}h_{sv} - C\frac{dh_{sv}}{d\theta}\right] \\
&\frac{d\varphi}{d\theta} = -\frac{\left[\frac{1}{2}\omega k\varphi V_h\sin\theta + \frac{\lambda}{4}\omega\varphi kV_h\sin 2\theta - \varphi^{\frac{1}{k}}\alpha_v\pi d_{sv}h_{sv}\sqrt{\frac{2kRT_s}{k-1}}\sqrt{1-\varphi^{\frac{k-1}{k}}}\right]}{\omega V_h(\xi+\frac{1}{2}-\frac{1}{2}\cos\theta+\frac{\lambda}{4}\sin^2\theta)}
\end{aligned}\right\} \quad (21)$$

CALCULATION PROCEDURE

The simulation is implemented in a MATLAB environment for an efficient numerical solution. The Fourth order Runge-Kutta method is adopted to solve the models because of its high precision (Wang Y *et al*., 2013).

Initial conditions

The initial angle θ_0 is the instantaneous crank angle of the reed valve, which is moved away from the valve seat. Three initial conditions of the discharge valve and suction valve can be expressed as equation 22 and equation 23:

$$\text{Discharge valve: } \left(\frac{dh_{dv}}{d\theta}\right)_{\theta_{d0}} = 0,\ \left(\frac{d^2h_{dv}}{d\theta^2}\right)_{\theta_{d0}} = 0,\ (\psi)_{\theta_{d0}} = 1 + \frac{K_{dv}H_{d0}}{A_{dp}p_d} \quad (22)$$

$$\text{Suction valve: } \left(\frac{dh_{sv}}{d\theta}\right)_{\theta_{so}} = 0,\ \left(\frac{d^2h_{sv}}{d\theta^2}\right)_{\theta_{so}} = 0,\ (\varphi)_{\theta_{so}} = 1 - \frac{K_{sv}H_{s0}}{A_{sp}p_s} \quad (23)$$

where θ_{d0} is the crank angle when the discharge valve opens, H_{d0} is the discharge valve lift , A_{dp} is the flow area of the discharge valve channel, θ_{s0} is the crank angle when the suction valve opens, H_{s0} is the suction valve lift, and A_{sp} is the flow area of the suction valve channel.

θ_{d0} and θ_{s0} can be calculated by equation 24 and equation 25, respectively:

$$\theta_{d0} = \arccos[1 - 2(1+\xi)\phi^{\frac{1}{n_g}} + 2\xi] \quad (24)$$

$$\theta_{s0} = \arccos[1 - 2\xi(\phi^{\frac{1}{m_g}} - 1)] \quad (25)$$

where ξ is the relative clearance volume of cylinder, ϕ is the ratio of discharge pressure to suction pressure, n_g is the gas compression process index, and m_g is the gas expansion process index.

The rebound coefficient of the reed valve (C_R) is the ratio between motion speeds before and after collision. $C_R = 0.25$.

Calculation procedure of the reed valve dynamics

The flow chart of the calculation procedure is shown in Figure 3. The dynamic model of the suction/discharge valve can be calculated according to the initial pressure ratio. The displacement curve, velocity curve, and pressure ratio curve can be obtained based on the calculation procedure.

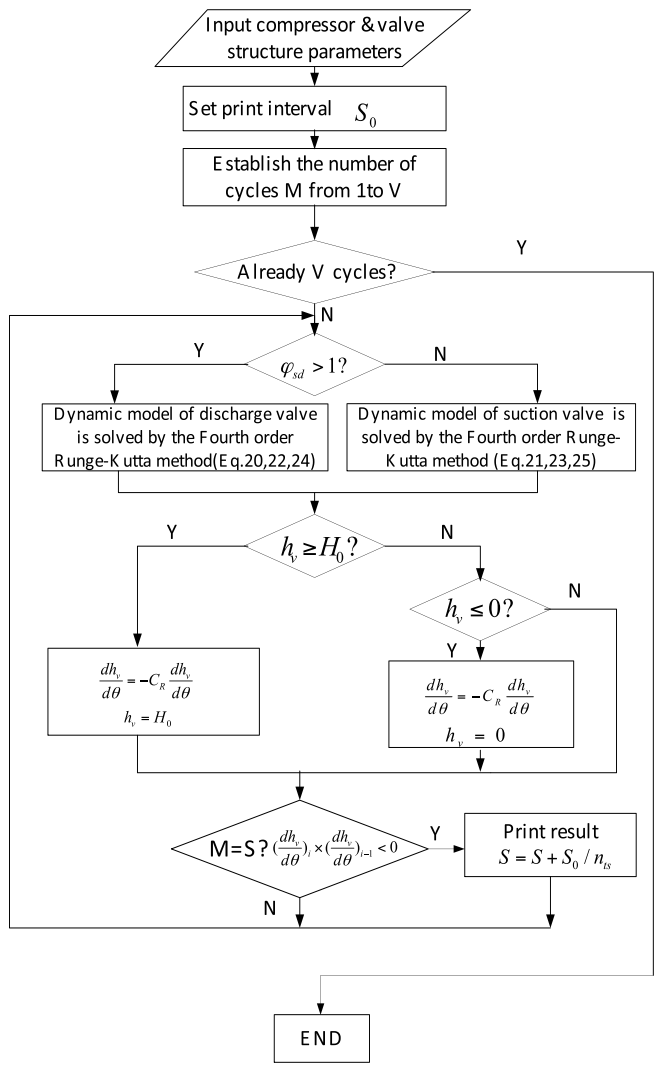

Fig. 3. The flow chart of the calculation procedure.

In Figure 3, S_0 is the set value of the print interval, S is the actual printing time, M is the actual cycle number, V is the set value of the maximum cycle number, φ_{sd} is the pressure ratio inside and outside the cylinder, h_v is the valve displacement, H_0 is the lift of the reed valve, and n_{ts} is the timestep.

The main parameters of the compressor and discharge valve are shown in Table 1.

Table 1. Main parameters of the compressor and discharge valve.

Main parameters of the compressor		**Main parameters of the discharge valve**	
Compressor speed[r/min]	1450	Quality of the valve[Kg]	0.00259
Cylinder diameter[m]	0.062	Valve lift[m]	0.0037
Cylinder stroke[m]	0.0484	Initial angle [°]	307
Relative clearance volume	2%	Valve width[m]	0.0174
Connecting rod length [m]	0.0996	Valve thickness[m]	0.00061
Suction temperature [K]	291	Effective valve length[m]	0.0037
Discharge temperature [K]	375	Elastic modulus [Pa (N/m^2)]	$2.1*10^{11}$
Suction pressure [Mpa]	0.296	Valve stiffness coefficient [N/ m]	4093
Discharge pressure [Mpa]	1.5	Valve gap flow coefficient	0.76
Crankshaft angular velocity [Rad/s]	151.77	Valve channel flow coefficient	0.52
Gas constant[J/Kg·K]	96.1	Flow area of valve channel [m^2]	0.000165
Crankshaft-connecting road ratio	0.23	Flow area of valve gap [m^2]	0.000104
Refrigerant	R22		
Evaporation temperature[°C]	-15~40		

EXPERIMENTS & CALCULATIONS COMPARISON

Experimental system

In order to measure the actual movements of the reed valve and evaluate the validity of the model, an experimental system of reciprocating compressor was established. The schematic diagram of experimental system is shown in Figure 4. The system is mainly composed of an evaporator, a reciprocating refrigeration compressor, a water-cooled condenser, a dry filter, a liquid storage tank, a temperature sensor, and so on.

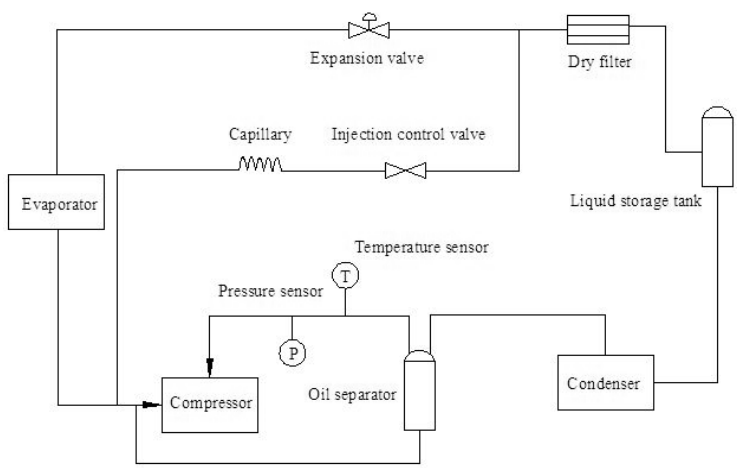

Fig. 4. The schematic diagram of the experimental system.

The displacement measurement system of the discharge valve is shown in Figure 5. The composition and parameters of the displacement measurement system are shown in Table 2.

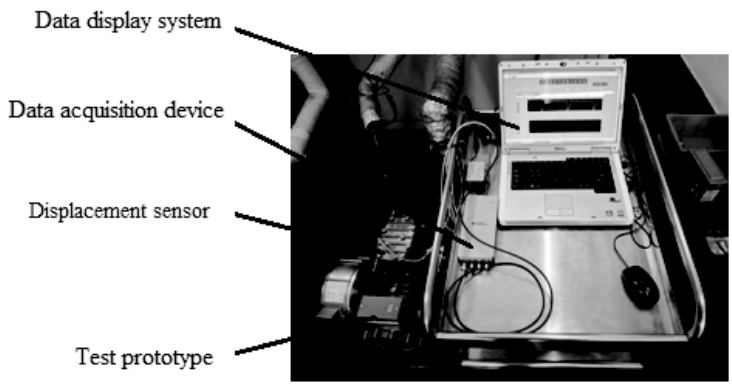

Fig. 5. Displacement measurement system of the discharge valve.

Table 2. Composition and parameters of the displacement measurement system.

System composition	Component parameters
Compressor power	5.5KW
Discharge valve thickness	0.61mm
Displacement sensor	ZA-21 eddy current displacement sensor
Data acquisition device	NI9230 data acquisition card
Data display software	Labview2015 data processing software

Experimental results & calculation results comparison

The experimental results and calculation results of the discharge valve displacement are shown in Figure 6. It can be seen from Figure 6 that the experimental results are in good agreement with the calculated results in the process of reed opening and fully open period. There is a rebound in closing process of the calculation results. It may be caused by viscous effect of oil film, which is not considered in the model.

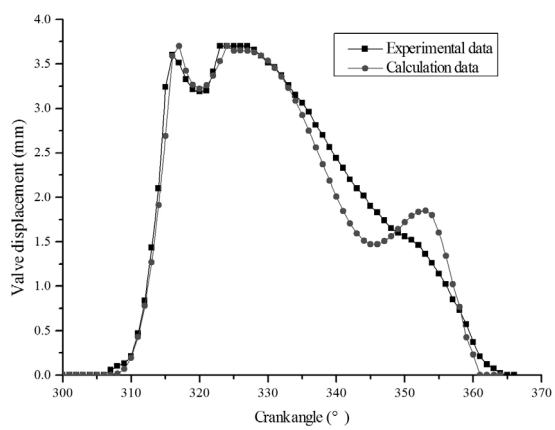

Fig. 6. Experimental results and calculation results of the discharge valve displacement.

Figure 7 shows the deviation between calculation results and experimental results of the discharge valve displacement. The majority of the calculated values fall within ±10% times error band. Therefore, the motion characteristics of the discharge valve can be effectively analyzed by the model.

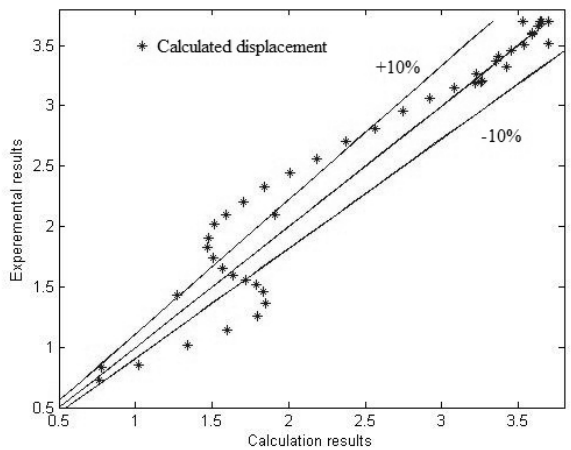

Fig. 7. Comparison of experimental results and calculation results of the discharge valve displacement.

CALCULATION RESULTS AND DISCUSSION

Effect of lift on the motion of the reed valve

The displacements of the discharge valve for different lifts are calculated when the compressor speed is 1450r/min and the valve stiffness coefficient is 4093N/m. Figure 8 shows the displacement curves of the discharge valve for different lifts.

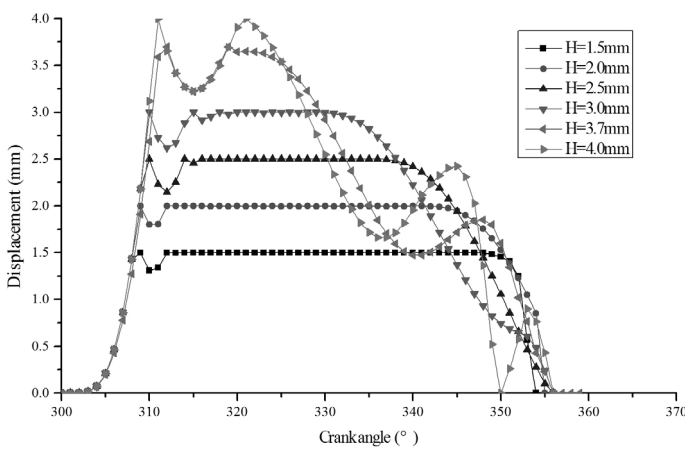

Fig. 8. Displacement curves of the discharge valve for different lifts.

Figure 8 shows that, with the increase of the lift, the rebound displacement after the discharge valve hitting the limiter is increased, and the fully open period is shortened. The rebound occurs during the valve falling back to the seat when the lift is 3.7mm. Thus, the valve lift cannot be set too high, which will cause rebound fluctuations, or even flutter. The area enclosed by displacement curve and abscissa represents the total flow area. The smaller the total flow area is, the greater the discharge loss is. Therefore, the valve lift cannot be set too low neither since it can lead to the increase of discharge losses.

The pressure ratio curves of the discharge valve for different lifts are shown in Figure 9. Figure 9 shows that, with the increase of the lift, the flow area of the valve channel outlet increases, the pressure in the cylinder decreases rapidly, and the pressure loss decreases.

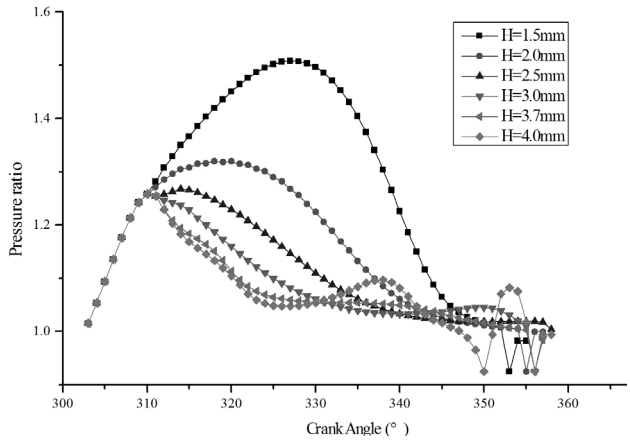

Fig. 9. Pressure ratio curves of the discharge valve for different lifts.

The relationship between impact velocity and valve lifts is shown in Figure 10. It can be found that when the lift is increased from 1.5mm to 3mm, the impact speed increases linearly. When the lift is higher than 3.7mm, the impact speed increases rapidly again. When the lift is 3mm ~3.7mm, the impact speed increases slowly. Therefore, the reasonable valve lift range is 3mm ~ 3.7mm according to the analysis above.

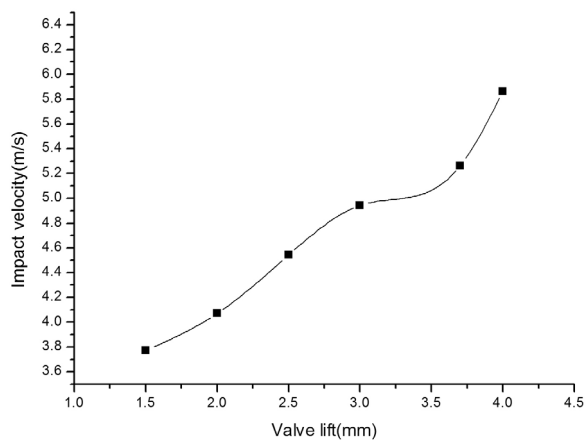

Fig. 10. The relationship between impact velocity and valve lifts.

Effect of stiffness coefficient on the motion of the reed valve

The elastic force (F_{sp}) can be calculated by equation 26:

$$F_{sp} = \frac{Eb\mu^3 l_{os}}{4L_A^3} \tag{26}$$

where E is the elastic modulus, b is the valve width, μ is the valve thickness, l_{os} is the feature lift, and L_A is the working length of valve.

The stiffness coefficient was calculated according to equation 26 and equation 16 when the valve lift is 3.7mm. The stiffness coefficients of different valve thickness are shown in Table 3.

Table 3. The stiffness coefficients of different valve thickness.

Valve thickness (mm)	0.51	0.56	0.61	0.66	0.71	0.81
Stiffness coefficient (N/m)	2392	3167	4093	5184	6454	9584

The displacement curves of the discharge valve for different stiffness coefficient are shown in Figure 11. It can be seen from Figure 11 that, with the increase of the stiffness coefficient, the opening time of the valve reed is delayed, the initial closing angle is reduced significantly, and the fully open period is reduced severely.

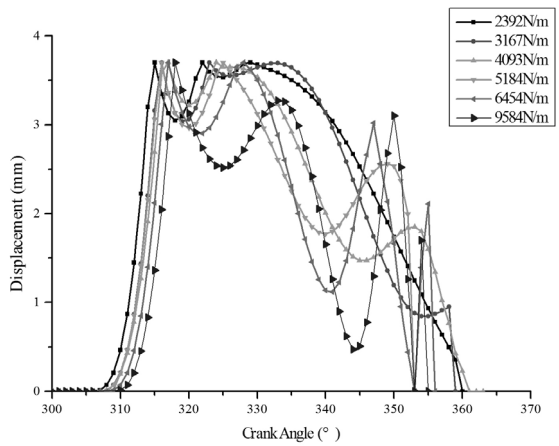

Fig. 11. Displacement curves of the discharge valve for different stiffness coefficients.

The speed curves of the discharge valve for different stiffness coefficients are shown in Figure 12, which presents that, with the increase of the stiffness coefficient, the impact speed of the valve is reduced. When the stiffness coefficient is greater than 5000 N/m, the fluctuation of the valve is increased steeply and even leads to flutter. The discharge volume and working efficiency of the compressor are reduced. Therefore, the discharge valve thickness cannot be designed larger than 0.66mm for this compressor.

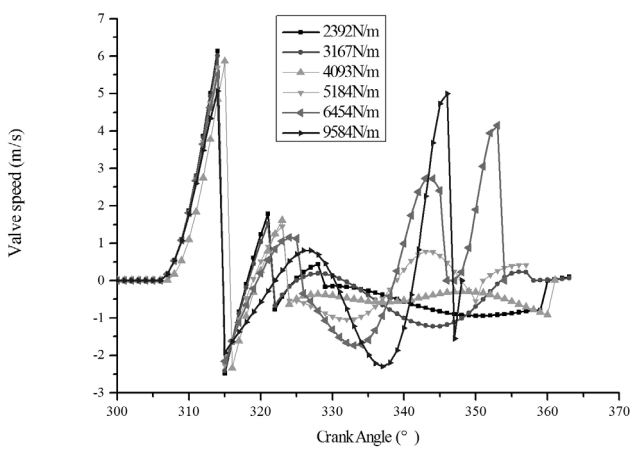

Fig. 12. Speed curves of the discharge valve for different stiffness coefficients.

Effect of effective flow area on the motion of the reed valve

The effective flow area is directly related to valve lift and orifice diameter. The displacement curves of the discharge valve for different orifice diameters are shown in Figure 13. It can be found that, with the decrease of the discharge orifice diameter, the full opening angle is increased and the closing angle of the valve tends to be prolonged. Due to the reduction of the effective flow area of the valve, the gas thrust is weakened.

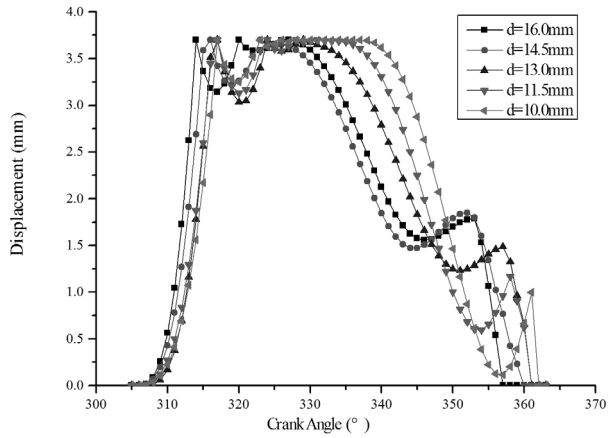

Fig. 13. Displacement curves of the discharge valve for different orifice diameters.

The pressure ratio curves of the discharge valve for different orifice diameters are shown in Figure 14, which shows that, with the decrease of the discharge orifice diameter, the pressure ratio is increased. In addition, the pressure ratio is rapidly increased again during the valve's falling back to seat, which will cause valve fluctuation. Thus, the flutter and pressure loss of the discharge valve can be reduced by increasing the valve effective flow area. However, when the orifice diameter is larger than 13.0mm, the fully open period is sharply shortened. Therefore, the valve effective flow area cannot be enlarged only by increasing the orifice diameter.

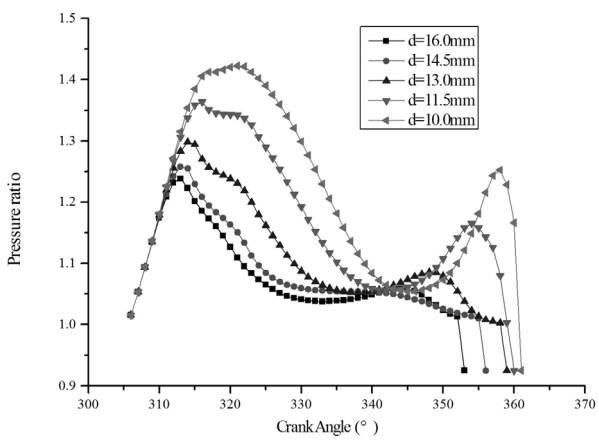

Fig. 14. Pressure ratio curves of the discharge valve for different orifice diameters.

CONCLUSIONS

A dynamic model of the reed valve is established in this paper. The structural parameters of the reed valve and the gas damping force are considered in this new model. Afterwards, the dynamic model of the discharge valve is solved by the Fourth order Runge Kutta method in MATLAB environment.

The displacement measurement system of the discharge valve is established in order to evaluate the validity of the developed model. The calculated displacements can agree well with the experimental results. The motion characteristics of the discharge valve can be effectively analyzed by the model. Moreover, the effects of valve lift, stiffness coefficient and effective flow area on impact speed, fully open period, and fluctuation are explored based on the model.

ACKNOWLEDGMENT

This project is supported by the National Natural Science Foundation of China (Research Project 51205035) and Natural Science Foundation of Liaoning province (Research Project 201602133, Project 20170540107, and Project 20180550493).

REFERENCES

Bo Huang. 2008. Dynamic Analysis of the Discharge Valve of the Rotary Compressor. International Compressor Engineering Conference. Purdue University. article 1182.

Costagliola, M. & Great Neck, N.Y. 1950. The Theory of Spring-Loaded Valves for Reciprocating Compressors. Journal of applied mechanics, **17**(4): 415-420.

Daniel Nagy. 2008. Valve Lift Measurement for the Validation of a Compressor Simulation Model. International Compressor Engineering Conference. Purdue University. article 1274.

Hong, W., Jin, J. & Wu, R. 2009. Theoretical analysis and realization of stepless capacity regulation for reciprocating compressors. Proceedings of the Institution of Mechanical Engineers, Part E: Journal of Process Mechanical Engineering, **223**(4): 205-213.

Junghyoun Kim. 2006. Valve Dynamic Analysis of a Hermetic Reciprocating Compressor. International Compressor Engineering Conference. Purdue University. article C107.

Lawson S. & Mclaren R.J.L. 1984. Approach to Computer Modeling of Reciprocating Compressors. Proceedings of the Purdue Compressor Technology Conference. Purdue University pp. 139-147.

Lin Mei, YaoJun & Pan shulin. 1997. Establishment of three mathematical models and comparison for the reed valves. Chinese Journal of Applied Mechanics, **14**(1):118-123.

Machu, E. 2001. Valve dynamics of reciprocating compressor valves with more than one degree of freedom. Proceedings of the ImechE. pp:1385-1392.

Shuhei NAGATA. 2010. Analysis of Dynamic Behavior of Suction Valve Using Strain Gauge in Reciprocating Compressor. International Compressor Engineering Conference at Purdue University. article 1273.

Soedel Werner. 1972. Introduction to Computer Simulation of Positive Displacement Type Compressors. Proceedings of the 1972 Purdue Compressor Conference: Short Course, West Lafayette, Indiana, USA.

Soedel Werner. 1984. Design and Mechanics of Compressor Valves. Proceedings of the 1984 International Compressor Conference at Purdue: Short course, West Lafayette, Indiana, USA.

Feng Wang, Guangyu Mu & Qiang Guo. 2016. Design optimization of compressor reed valve based on axiomatic design. International journal of refrigeration, **72**: 132–139.

Wang Y, Xue C & Feng J. 2013. Experimental investigation on valve impact velocity and inclining motion of a reciprocating compressor. Applied Thermal Engineering, **61**(2):149-156.

Wambsganss, M.W. 1966. Mathematical Modeling and Design Evaluation of High-Speed Reciprocating Compressors. PHD Thesis, Purdue University.

Wu danqing & Cong jingtong. 1993. Mathematical simulation and design of compressor reed valve. Mechanical Industry Press. Beijing.

Yuan Ma, Zhilong He, Xueyuan Peng & Ziwen Xing. 2012. Experimental investigation of the discharge valve dynamics in a reciprocating compressor for trans-critical CO2 refrigeration cycle, Applied Thermal Engineering, **32**: 13-21.

Submitted: 20/10/2016
Revised: 18/01/2017
Accepted: 09/05/2019

نمذجة صمامات الزنبرك في الضواغط الترددية ودراسة الخصائص الديناميكية لها

،*قوانغ مو، ***فنغ وانغ و****شياوتشين مي
*كلية الهندسة الميكانيكية والطاقة، جامعة داليان أوشن، داليان، الصين
**كلية الهندسة الميكانيكية، جامعة داليان جياوتونغ، داليان، الصين
***كلية موتور تران، جامعة داليان جياوتونغ، داليان، الصين
****كلية المرور والنقل، جامعة داليان جياوتونغ، داليان، الصين

الخلاصة

من أجل دراسة الخصائص الديناميكية لصمامات الزنبرك في الضواغط الترددية، تم في هذه الدراسة تطوير نموذج جديد قائم علي الحفاظ على الطاقة وقانون نيوتن الثاني للحركة. ففي هذا النموذج الجديد، تم الأخذ في الاعتبار المعلمات الهيكلية لصمامات الزنبرك وقوة تخميد الغاز. وعلاوة على ذلك، تم إنشاء نظام تجريبي للضاغط الترددي لقياس الحركات الفعلية لصمامات الزنبرك ولتقييم صلاحية النموذج. وتم تنفيذ المحاكاة في بيئة MATLAB للتوصل إلى الحل الرقمي الفعال وعرض النتائج. وكانت النتائج التجريبية متسقة مع نتائج المحاكاة الرقمية والتي أظهرت أن النموذج النظري المُقترح فعال ودقيق. وعلاوة على ذلك، تستخدم هذه الدراسة أيضاً هذا النموذج لتحليل تأثير المعلمات الهيكلية على الخصائص الديناميكية والحصول على نطاق معقول لمعلمات التصميم. وعملياً، يمكن لهذا البحث أن يصبح مرجعاً مفيداً للتصميم الأمثل لصمامات الزنبرك.